

# Cancer-associated fibroblasts promote PD-L1 expression in mice cancer cells via secreting CXCL5

Ziqian Li<sup>1</sup>, Jiawang Zhou<sup>1</sup>, Junjie Zhang<sup>1</sup>, Shiyang Li<sup>2</sup>, Hongsheng Wang<sup>1</sup> and Jun Du<sup>1</sup>

<sup>1</sup>Department of Microbial and Biochemical Pharmacy, School of Pharmaceutical Sciences, Sun Yat-sen University, Guangzhou, China

<sup>2</sup>Department of Pharmacology, School of Pharmaceutical Sciences, Jinan University, Guangzhou, China

Cancer-associated fibroblasts (CAFs) play a key role in orchestrating the tumor malignant biological properties within tumor microenvironment and evidences demonstrate that CAFs are a critical regulator of tumoral immunosuppression of the T cell response. However, the functions and regulation of CAFs in the expression of programmed death-ligand 1 (PD-L1) in melanoma and colorectal carcinoma (CRC) are not completely understood. Herein, by scrutinizing the expression of  $\alpha$ -SMA and PD-L1 in melanoma and CRC tissues, we found that CAFs was positive correlated with PD-L1 expression. Further analyses showed that CAFs promoted PD-L1 expression in mice tumor cells. By detecting a majority of cytokines expression in normal mice fibroblasts and CAFs, we determined that CXCL5 was abnormal high expression in CAFs and the immunohistochemistry and *in situ* hybridization confirmed that were CAFs which were expressing CXCL5. In addition, CXCL5 promoted PD-L1 expression in B16, CT26, A375 and HCT116. The silencing of CXCR2, the receptor of CXCL5, inhibited the PD-L1 expression induced by CAFs in turn. Functionally, CXCL5 derived by CAFs promoted PD-L1 expression in mice tumor cells through activating PI3K/AKT signaling. LY294002, the inhibitor of PI3K, confirmed that CXCL5 forested an immunosuppression microenvironment by promoting PD-L1 expression via PI3K/AKT signaling. Meanwhile, the B16/CT26 xenograft tumor models were used and both CXCR2 and p-AKT were found to be positively correlated with PD-L1 in the xenograft tumor tissues. The immunosuppressive action of CAFs on tumor cells is probably reflective of them being a potential therapeutic biomarker for melanoma and CRC.

**Key words:** CXCL5, CAFs, PD-L1, melanoma, colorectal cancer

**Abbreviations:** CAFs: cancer-associated fibroblasts; CCL: C-C motif chemokine ligand; CRC: colorectal cancer; CXCL: C-X-C motif chemokine ligand; CXCR: C-X-C motif chemokine receptor; HRP: horseradish peroxidase; IFN- $\gamma$ : interferon- $\gamma$ ; IHC: immunohistochemistry; ISH: *in situ* hybridization; PD-L1: program death-ligand 1; TNF: tumor necrosis factor;  $\alpha$ -SMA:  $\alpha$ -smooth muscle actin

Additional Supporting Information may be found in the online version of this article.

**Conflict of interest:** The authors state no conflict of interest.

**Grant sponsor:** National Natural Science Foundation of China;

**Grant numbers:** 81472643 and 81672943

**DOI:** 10.1002/ijc.32278

This is an open access article under the terms of the Creative Commons Attribution-NonCommercial-NoDerivs License, which permits use and distribution in any medium, provided the original work is properly cited, the use is non-commercial and no modifications or adaptations are made.

**History:** Received 14 Sep 2018; Accepted 13 Mar 2019; Online 15 Mar 2019.

**Correspondence to:** Jun Du, Department of Microbial and Biochemical Pharmacy, School of Pharmaceutical Sciences, Sun Yat-sen University, No. 132 Waihuan East Road, University Town, Guangzhou 510006, China, E-mail: dujun@mail.sysu.edu.cn

## Introduction

Melanoma and colorectal cancer (CRC) are common cancers associated with high mortality worldwide.<sup>1</sup> The management of melanoma and CRC have improved overall survival rates during the last decades, yet the majority of patients do not respond to treatment and succumb to disease progression, mainly due to upregulating the surface program death-ligand 1 (PD-L1) expression.<sup>2–4</sup> Therefore, deep understanding of the PD-L1 upregulating mechanism is urgently needed for melanoma and CRC.

The tumor microenvironment is shown to be composed of extracellular matrix and stromal cells, such as cancer-associated fibroblasts (CAFs), the main cell types constituting the tumor stroma.<sup>5,6</sup> Emerging evidence has shown that CAFs are critical for remodeling the tumor microenvironment and ultimately affect tumor initiation and progression.<sup>7,8</sup> Aberrant secretion of cytokines to tumor site is one of the features of CAFs. It is acknowledged that cytokines serve as mediators in shaping tumor microenvironment and facilitating tumor progression.<sup>9,10</sup> Previous studies have reported that C-X-C motif chemokine ligand 12 (CXCL12), interferon- $\gamma$  (IFN- $\gamma$ ), CXCL9/10/11 and IL6 promoted PD-L1 expression in cancer cells.<sup>11–14</sup> In this regard, we postulated that CAFs-derived cytokines might promote PD-L1 expression.

**What's new?**

Cancer-associated fibroblasts (CAFs) play a key role in orchestrating tumor malignant properties within the tumor microenvironment. However, the role of CAFs in tumor PD-L1 expression and immune evasion in melanoma and colorectal carcinoma (CRC) is not completely understood. Here, the authors observe a positive correlation between CAFs and PD-L1 expression in patients. CAFs promote PD-L1 expression in tumor cells by secreting CXCL5 and in turn activating the PI3K/AKT signaling pathway. The findings reveal a complex tumor-promoting microenvironment shaped by the CXCL5-CXCR2 axis and highlight CAFs as a promising target to curb immune evasion.

After discovering the positive correlation between CAFs and PD-L1 expression, we isolated and enriched the CAFs in mice tumor models and then scrutinized the expression of most cytokines in CAFs, identifying CXCL5 as the abundant expression of cytokines. Notably, CXCL5 promoted PD-L1 expression in melanoma and CRC cells via PI3K/AKT signaling pathway. Blockade of CXCL5–C-X-C motif chemokine receptor 2 (CXCR2) axis reduced PD-L1 expression *in vitro*, representing a promising therapeutic method.

**Materials and Methods****Tissue samples and histological study**

The human melanoma and CRC cancer tissues were obtained from the First Affiliated Hospital of Clinical Medicine of Guangdong Pharmaceutical University in Huizhou, China. The studies were got the approval by the Ethical Committee of Pharmaceutical Sciences, Sun Yat-sen University under the Chinese Ethical Regulations.

Immunohistochemistry (IHC) was used to measure the expression of PD-L1 and  $\alpha$ -SMA as reported previously.<sup>15</sup> In short, we deparaffinized, hydrated and blocked the sections with 3% H<sub>2</sub>O<sub>2</sub> for 20 min. Slides were then blocked with normal goat serum for 1 hr after high pressure antigen retrieval in citric acid buffer (pH = 6.0) for 10 min and incubated overnight at 4°C with antibodies. After incubation with the appropriate horseradish peroxidase (HRP)-conjugated antibodies (1:200, Bioworld Technology, St. Louis Park, MN) for 2 hr, the signals were observed with a Diaminobenzidine kit, stained with hematoxylin. The specimens were observed with microscope. The following antibodies were used for IHC, flow cytometry and western blotting: rabbit monoclonal anti-PD-L1 (1:200, ab205921, Abcam, Cambridge, MA), mouse monoclonal anti- $\alpha$ -smooth muscle actin ( $\alpha$ -SMA; 1:200, BM0002, BOSTER Biological Technology, Pleasanton, CA), rabbit polyclonal anti-CXCR2 (1:200, BA0732-2, BOSTER).

Masson trichrome staining was executed using Masson Staining Kit (Wanleibio, Shenyang, China) for tumor tissue samples according to their manufacturer's protocol.

The localization of CXCL5 in human CRC tissue was observed by *in situ* hybridization (ISH), respectively. 4- $\mu$ m sections of samples with a digoxigenin-labeled oligonucleotide CXCL5 detection probe were analyzed in BersinBio, Guangzhou, China. CXCL5 probe was 5'-CCA GTG ATT CCT GGC TCA CAC TAT AGT CAA TTG CCA AAA CTT CAA TAG CAT AGC AGA TAA AAT AAC AGC AAA TAG CAG

AGG TAC TAT GCT AAA CAC TTC ATT AGC TGA GCT GAA AGC TTA AGC GGC AAA CAT AGG TTT TCC TCA CAC TCT TCA AAG TGA GGA ATC CAG GAA GAA AGC TAA CTA CTG GAA AAA CAA ATA AAC AAA CAA CAA CAA AAT CTT TCC TTC TTG TCT TCC CTG GGT TCA GAG ACC TCC AGA-3'.

**Evaluation of IHC staining**

Three independent scorers (JZ, JZ and SL) observed the stained specimens and recorded the scores by assessing (a) the proportion of positively cells per the whole cells (0, <5%; 1, 6–25%; 2, 26–50%; 3, 51–75%; 4, 76–100%) and (b) the intensity of staining (0, negative; 1, weak staining; 2, medium staining; 3, strong staining). The score was calculated by  $a \times b$ .

**Cell cultures**

Mouse fibroblast (3T3), mouse melanoma (B16), mouse CRC (CT26), human melanoma (A375) and human CRC (HCT116) cell lines were bought from the Institute of Biochemistry and Cell Biology, Chinese Academy of Sciences (Shanghai, China). 3T3, B16 and CT26 were maintained in Dulbecco's modified Eagle medium (DMEM; GIBCO-BRL, Gaithersburg, MA) supplemented with 10% FBS at 37°C incubator under a humidified 5% CO<sub>2</sub> atmosphere. A735 and HCT116 were cultured in RPMI-1640 medium supplemented with 10% FBS.

Primary murine CAFs were isolated from the subcutaneous xenograft tissues, constructed by  $5 \times 10^6$  B16 in C57BL/6 for 7 days, with ethical approval. Two 4- to 5-week-old female C57BL/6 mice were provided by the Animal Experimental Center of Sun Yat-sen University (Guangzhou, China) and housed in the Laboratory Animal Center under specific pathogen-free conditions. The experimental handling and care procedures for the mice were got the approval from the Animal Experimentation Ethics Committee of Sun Yat-sen University (Guangzhou). Primary murine CAFs were detached and cultured in DMEM supplemented with 10% FBS. The different monoclonal of CAFs were named as CAF1, CAF2, CAF3, CAF4, CAF5 and CAF6, respectively. All cell cultures were routinely tested for mycoplasma contamination.

**Cell transfection and the generation of B16-GFP and CT26-GFP cells**

Cells were plated in six-well plates at a density of  $10^5$  cells per plate with 2 ml culture medium and incubated for 12 hr before transfected. The pGFP-V-RS plasmid with GFP was purchased

from Origene (TR TG501492, Origene Technologies, Rockville, MD) and transfected into B16 and CT26 cells with Lipofectamine 3000 (Invitrogen, Carlsbad, CA) according to their manufacturer's protocols. Stable transfectants were selected with puromycin (2 µg/ml) and the survived cells were passaged for cell clones formation and further expansion.

The pGFP-CXCL5 plasmid and the corresponding mock plasmid, purchased from Addgene (Cambridge, MA), were transfected into 3T3 cells respectively with Lipofectamine 3000 according to the supplier's protocol. The cells transfected with mock plasmid were called 3T3-mock and the other was 3T3-CXCL5. The siRNA specific for the mouse CXCR2 mRNA (5'-GCTATGAGGATGTAGGTAA-3') and human CXCR2 mRNA (5'-CGCTACTTGGTCAAATTC-3') were designed and synthesized by RiboBio Co., Ltd (Guangzhou, China).

### Flow cytometric analyses

Cells ( $1 \times 10^6$ ) were collected in eppendorf and incubated with the appropriate antibodies in room temperature for 30 min. After washing by PBS, the appropriate FITC or DyLight 649-conjugated antibodies were used to combine with the first antibodies and the fluorescence was analyzed by flow cytometric analysis following the protocol.

### Gene expression heatmap

Cells were subjected to Trizol (Invitrogen), qRT-PCR was studied by Prime Script™ RT reagent Kit (R036A; Takara, Japan) and SYBR Premix Ex Taq™ II (R820A; Takara, Japan). General principles of primers used in our researches were designed in the Genbank database. The utilized primers are listed in Supporting Information Table S1. The threshold cycle values in every sample were normalized as the values of GAPDH. The relative fold changes were figured up with the comparative threshold cycle method. The fold-changes differences in mRNA expression level were constructed in the heatmap using OmicShare Platform with sample clustering.

### The slides of cells and immunofluorescence

A total of  $3 \times 10^5$  CAFs or 3T3 cells were passaged on the coverslips in six-well plates for 12 hr. The coverslips were collected and cells were fixed by 4% paraformaldehyde. After blocked with 3% H<sub>2</sub>O<sub>2</sub> for 20 min, slides were blocked by normal goat serum for 1 hr and incubated with CXCL5 antibody at 4°C overnight. Coverslips were incubated with FITC-conjugated antibody and stained by 4', 6-diamidino-2-phenylindole (DAPI; Invitrogen). The slips were observed with an Olympus FV3000 microscope (Japan).

Briefly, the 4-µm section of human CRC tissue samples were deparaffinized, hydrated and blocked with 3% H<sub>2</sub>O<sub>2</sub>. Sections were then blocked with normal goat serum after high-pressure antigen retrieval in citric acid buffer and incubated at 4°C overnight with CXCL5 antibody and α-SMA antibody. After incubation with the appropriate FITC/DyLight

649-conjugated antibodies at room temperature in dark, the sections were stained by DAPI. Specimens were observed by an Olympus FV3000 microscope after added antifade reagent and covered with slides.

### Western blotting

Western blotting assay was performed as previously described<sup>15</sup> with antibodies against CXCL5, AKT, p-AKT, PI3K, p-PI3K (Cell Signaling Technology, Danvers, MA), α-tubulin (Bioworld Technology, St. Louis Park, MN).

### Xenograft tumor models

In total,  $5 \times 10^6$ /ml B16 cells injected into C57BL/6 mice subcutaneously under the right shoulder. The BALB/c mice were inoculated with CT26 cells subcutaneously, with ethical approval. Mice were bought from the Animal Experimental Center of Sun Yat-sen University and divided into five for each group. When the tumor grew to approximately 200 mm<sup>3</sup> for about 10 days, the subcutaneous tumors were collected and embedded in paraffin after fixation in formalin. Then, 4 µm sections of each mouse were cut for IHC analysis and evaluated as the method described above.

### Statistical analysis

The statistical analysis of our experiments was carried out on a minimum of three independent experiments. All statistical analyses were performed with IBM SPSS Statistics version 20 (IBM Corp., Armonk, NY) for Windows. Values of  $p < 0.05$  were considered as statistically significant. The unpaired two-tailed Student's *t*-test was used to analyze two groups and one-way ANOVA was used for multiple comparisons.

## Results

### Patient tumors express PD-L1, considerably corrected with expression of α-SMA

CAFs have been confirmed the complex interaction with tumor cells, including tumor immunosuppression.<sup>7</sup> We evaluated the association of PD-L1 and α-SMA expression in tumors. First, IHC was carried out to verify PD-L1 and α-SMA expression from 94 melanoma patients and 112 CRC patients' tumor tissues. We studied the relationship between α-SMA and PD-L1 expression. Among the patients, the expression of PD-L1 was notably correlated with the expression of α-SMA (Fig. 1). These findings from patient tumors indicated that CAFs possibly played an important role in moderate PD-L1 expression in tumor cells.

### CAFs promote PD-L1 expression in mice tumor cells

In order to identify the role of CAFs on PD-L1 expression, we isolated and enriched the CAFs in the mice subcutaneous xenograft tissues, as the protocol described in the methods section (Supporting Information Fig. S1A). Comparing 3 T3 cell lines, CAFs significantly expressed α-SMA (Fig. 2a and 2b), identified that CAFs were basically purified. We firstly tested

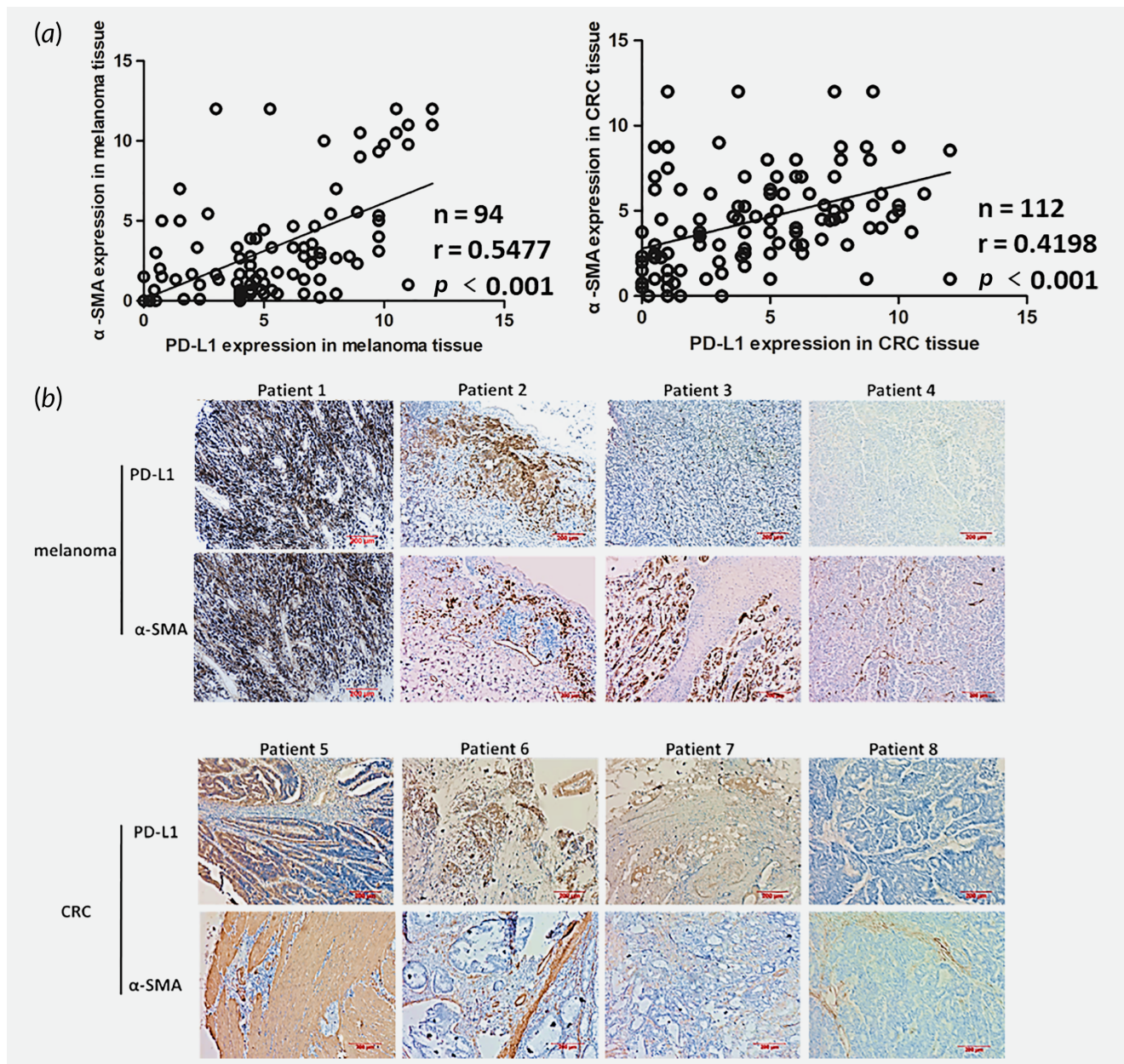


**Figure 1.** The expression of  $\alpha$ -SMA correlates with PD-L1 in human melanoma and CRC tissues. (a) The expression level of  $\alpha$ -SMA and PD-L1 in human melanoma and CRC tissues were detected by IHC and evaluated. (b) Representative immunostaining images of  $\alpha$ -SMA and PD-L1 in melanoma and CRC tissues. Scale bar, 200  $\mu$ m.

cocultures of melanoma cell line B16 or CRC cell line CT26 with CAFs by transwell insert and found a significant increase of PD-L1 expression in mice tumor cells (Fig. 2c). To further investigate the effect of CAFs, we generated the B16 and CT26 with GFP expression by plasmid editing (Supporting Information Fig. S1B) and tested their PD-L1 expression after cocultured with CAFs directly. Consistent with previous finding, PD-L1 expression showed a significant upregulated in the CAFs cocultured group (Fig. 2d). Altogether the data suggest that the CAFs cells in the tumor microenvironment stimulate PD-L1 expression in mice cancer cell lines.

#### CXCL5 is high expression in CAFs

Above finding prompted us to explore the potential mechanism(s) of PD-L1 upregulation by CAFs. Prior literature suggests that PD-L1 upregulated by some cytokines in tumor microenvironment, such as CCL15, IFN- $\gamma$ .<sup>12,16</sup> To determined which cytokines expressed in CAFs were different from normal fibroblasts, qRT-PCR was performed to scrutinize an amount of six CAFs cells. CXCL5, CXCL2, MMP3, and so on, were overexpressed cytokines in CAFs with the reference to normal fibroblasts cell lines 3T3 (Fig. 3a). Then, western blotting assay and immunofluorescence proved that the expression of CXCL5 was high

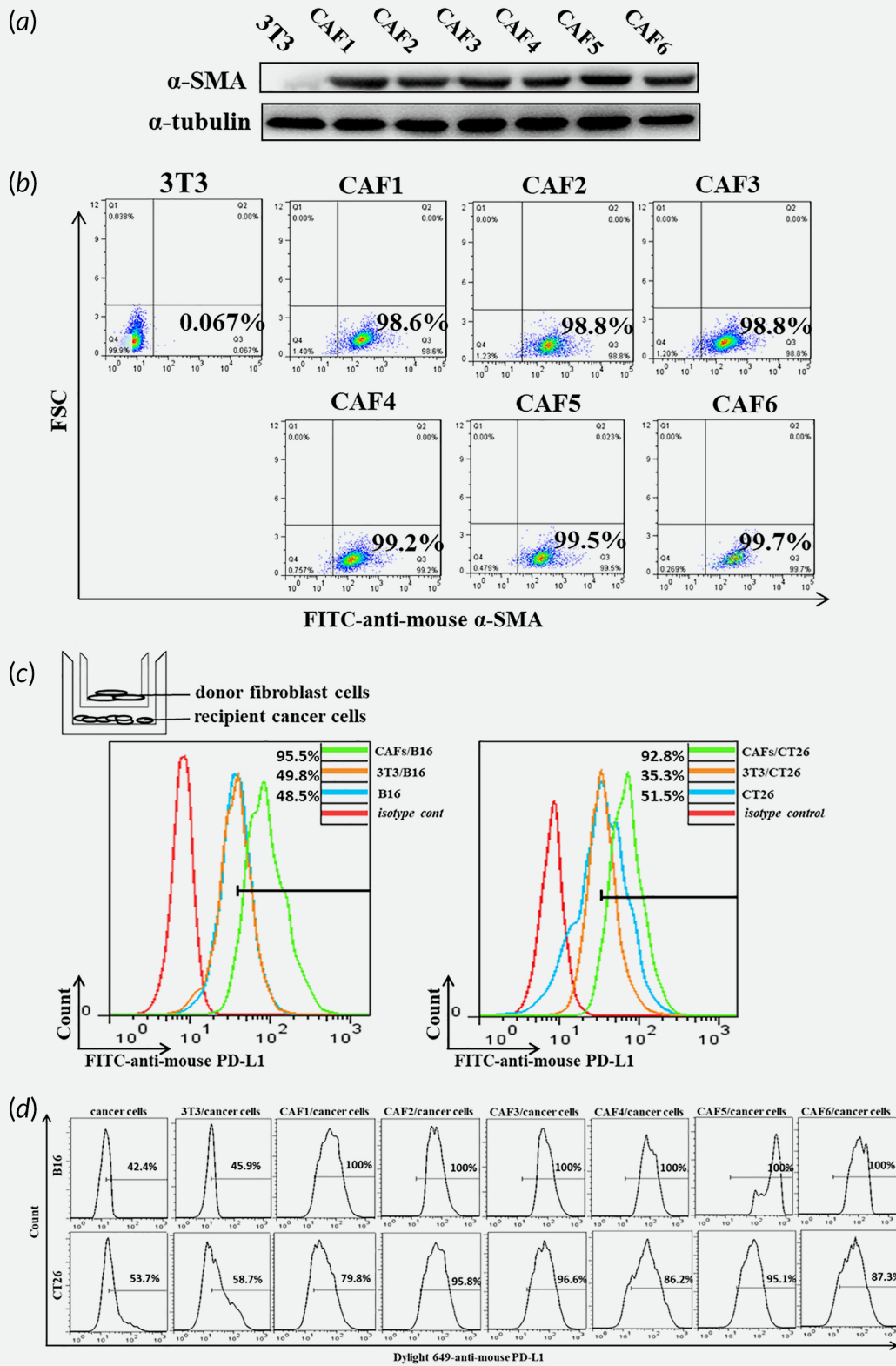


**Figure 2.** The CAFs isolated and enriched from the transplantation tumor promote PD-L1 expression in cancer cells. (a) The protein levels of  $\alpha$ -SMA in 3T3 and CAFs were detected by western blot. (b) The expression of  $\alpha$ -SMA in 3T3 and CAFs was detected by flow cytometry. (c) The diagram was showed the cocultured model and the expression of PD-L1 in tumor cells was detected by flow cytometry. (d) The expression of PD-L1 in tumor cells cocultured with fibroblasts directly was detected by flow cytometry.

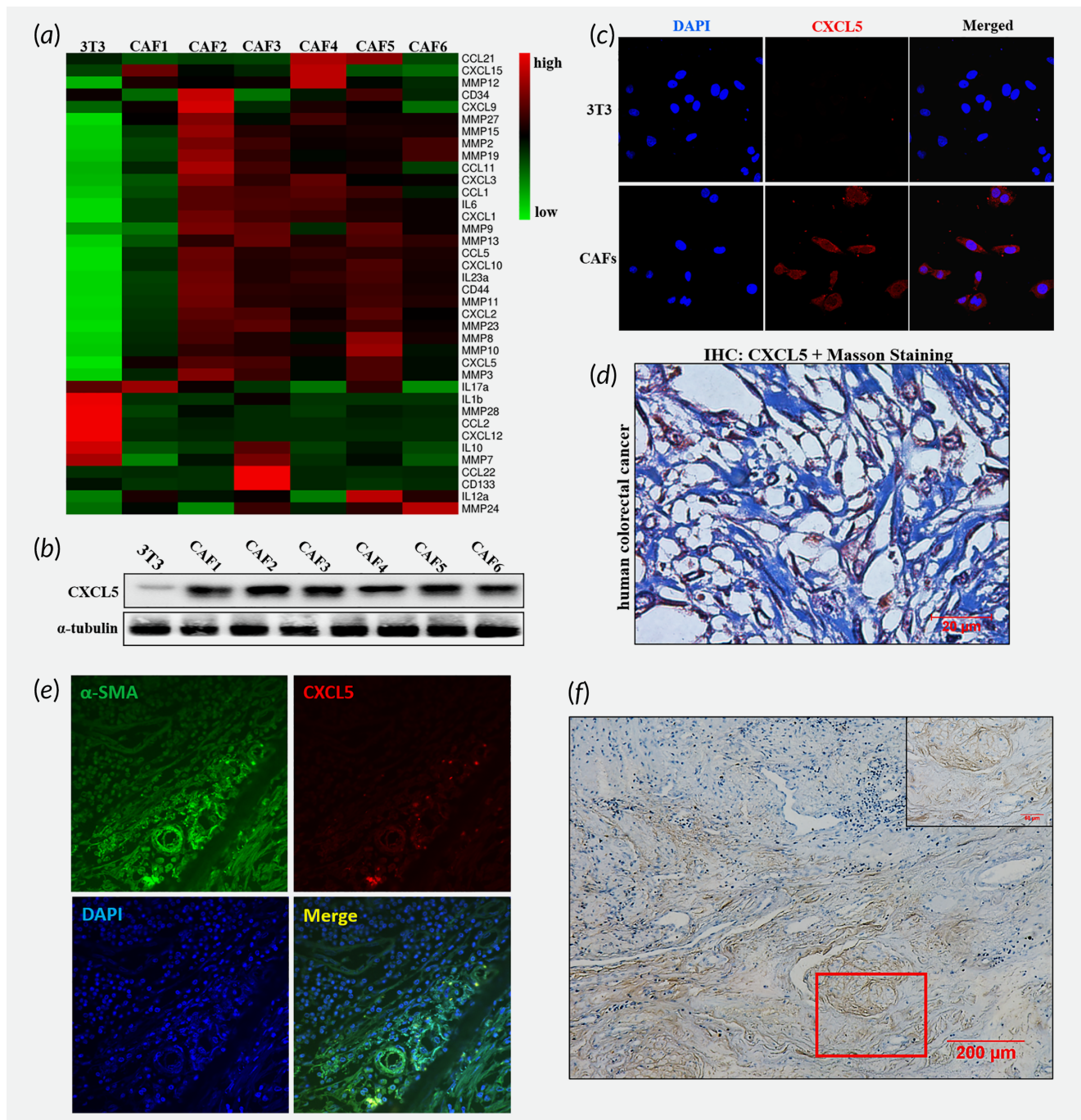


**Figure 3.** CXCL5 is significantly increased in CAFs compared to normal fibroblasts. (a) The differentially expressed genes between 3T3 and CAFs were shown in the heatmap by OmicShare Tool. (b) The protein level of CXCL5 in 3T3 and CAFs was showed by western blot analysis. (c) Immunofluorescence images showed CXCL5 expression in 3T3 and CAFs. (d) Representative immunostaining of CXCL5 and Masson's staining in human CRC tissues. (e) Representative images of immunofluorescence staining for  $\alpha$ -SMA and CXCL5 in human CRC tissues. (f) Representative images of ISH staining for CXCL5 in human CRC tissues (Scale bar, 200  $\mu$ m). The figure in the top right corner was the enlargement of the red rectangle square (Scale bar, 50  $\mu$ m).

in CAFs cell lines (Fig. 3b and 3c). Furthermore, the immunostaining and Masson's staining in the human CRC tissue showed that CAFs in tumor microenvironment expressed CXCL5 (Fig. 3d). In addition, the immunofluorescence and ISH in the human CRC tissue confirmed that were CAFs

which were expressing CXCL5 (Fig. 3e and 3f). Hence, we speculated that CXCL5 may play a significant role in PD-L1 expression in melanoma and CRC cells. Notably, other researches showed that serum CXCL5 concentration was significantly higher in nonsmall cell lung cancer patients than

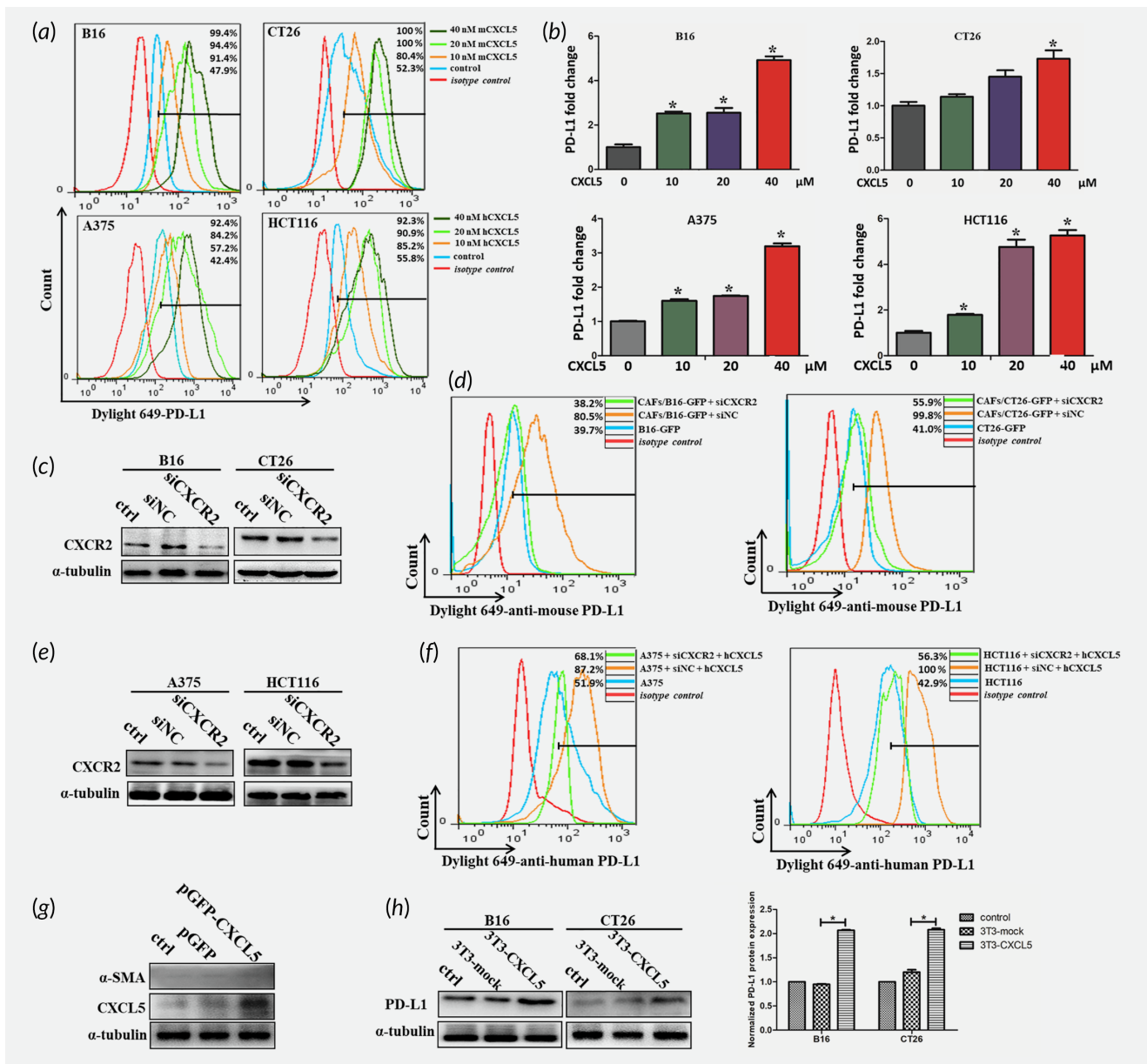


**Figure 4.** CAFs-derived CXCL5 promotes PD-L1 expression in cancer cells. (a) The expression of PD-L1 in B16, CT26, A375 and HCT116 was determined by flow cytometry after treated with different concentrations of recombinant CXCL5. (b) The mRNA expression of PD-L1 in B16, CT26, A375 and HCT116 was detected by RT-PCR.  $*p < 0.05$ . (c) Western blot showed the protein levels of CXCR2 in B16 and CT26 after transfected with siCXCR2. (d) Flow cytometry showed the expression of PD-L1 in B16 and CT26 cocultured with CAFs after transfected with siCXCR2. (e) The protein levels of CXCR2 in A375 and HCT116 after transfected with siCXCR2 were analyzed by western blotting. (f) The expression of PD-L1 in A375 and HCT116 treated with CXCL5 after transfected with siCXCR2 was determined by flow cytometry. (g) CXCL5 and  $\alpha$ -SMA expression in 3T3 cells were detected by western after transfected with CXCL5-overexpression plasmid. (h) PD-L1 protein expression in B16 and CT26 cocultured with/without 3T3-CXCL5 cells was analyzed by western blot and the normalized protein expression was analyzed by Image J.  $*p < 0.05$ .

those in healthy controls.<sup>12,16</sup> Those analyses have demonstrated that CXCL5 as a potential biomarker for cancers.

#### CAFs-derived CXCL5 promotes the expression of PD-L1 in cancer cells

Our next study was to explore the biological role of CXCL5 in increasing PD-L1 expression. Flow cytometry and qRT-PCR

analysis indicated that PD-L1 expression in B16, CT26, A375 and HCT116 was progressive increased after the treatment of CXCL5 at a gradient concentration (Fig. 4a and 4b). Considering that CXCL5 mainly and specifically bound to CXCR2, we silenced the expression of CXCR2 in B16 and CT26 (Fig. 4c). The expression of PD-L1 upregulated by CAFs was reversed by the silencing CXCR2 in tumor cells (Fig. 4d).

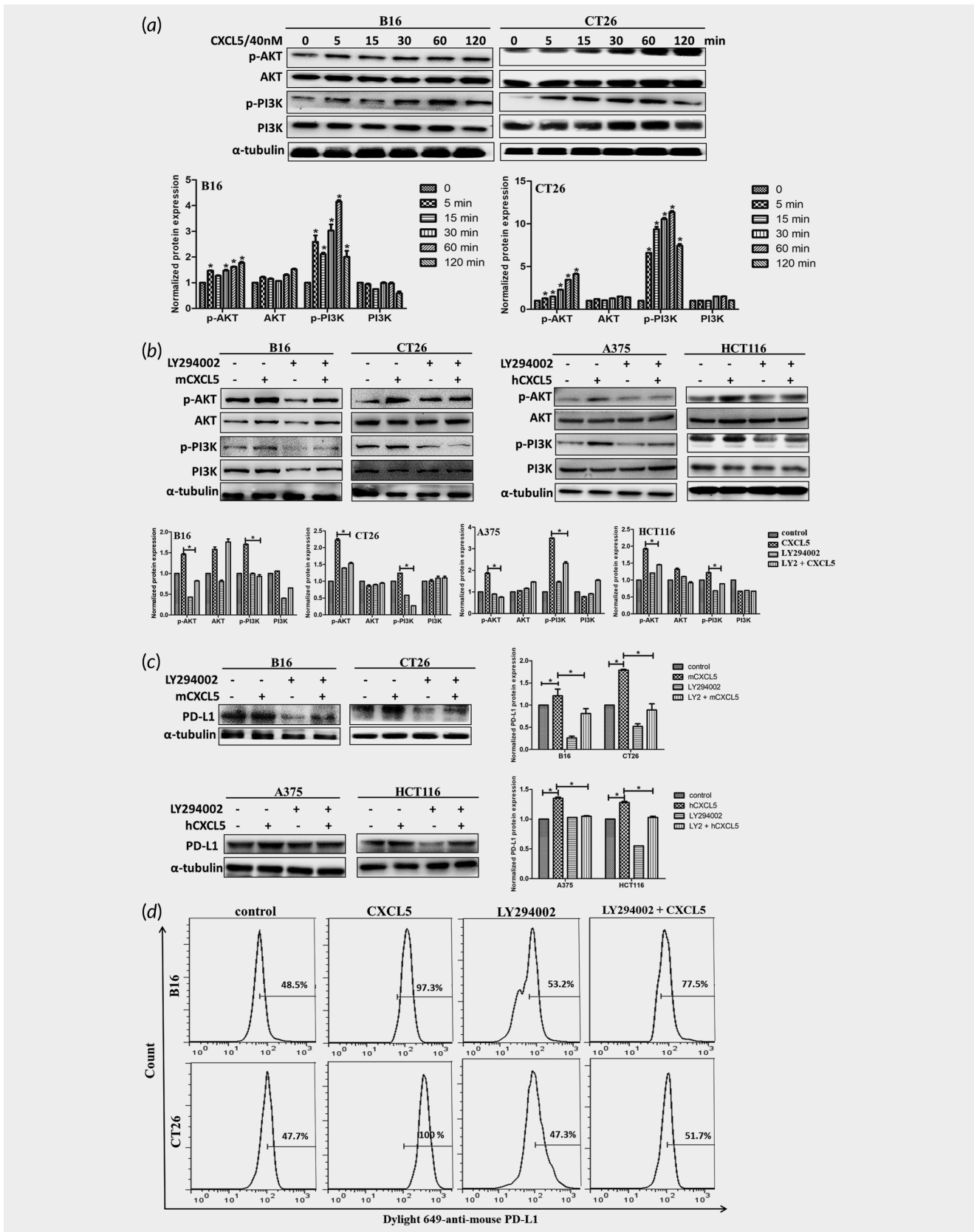


Figure 5. Legend on next page.



Similarly, for A375 and HCT116, the silencing expression of CXCR2 significantly reversed PD-L1 upregulated by CXCL5 (Fig. 4e and 4f). To confirm the effect of CXCL5 in PD-L1, 3T3 cells were transfected CXCL5-overexpressed plasmid and cocultured with B16 and CT26. The results showed that the CXCL5-overexpressed fibroblasts did not display CAFs properties (Fig. 4g). Identically, under the fibroblasts' activation with TGF- $\beta$ , a significant increase of  $\alpha$ -SMA in 3T3 was observed while the expression of CXCL5 did not change (Supporting Information Fig. S2). However, the expression of PD-L1 in B16 and CT16 was upregulated after cocultured with 3T3-CXCL5 (Fig. 4h). Those preliminary findings indicated that CXCL5 derived by CAFs was an effective cytokines to mediate PD-L1 upregulation.

### CXCL5 induces activation of PI3K and AKT to increase PD-L1 expression in melanoma and CRC cell lines

In subsequent researches, we wanted to find the underlying mechanism by which CAFs influenced CXCL5 mediated the expression of PD-L1. Previous researches have been reported that the oncogenic activation of RAS, AKT or TGF- $\beta$  signaling pathways control PD-L1 expression in numerous cancers.<sup>12,18,19</sup> We examined the total and phosphorylation levels of PI3K and AKT. PI3K and AKT were significantly phosphorylated in response to CXCL5 (Fig. 5a), implying CXCL5 activated the PI3K/AKT signal pathway. To confirm whether CXCL5-induced the expression of PD-L1 relied on activation of PI3K/AKT signaling, the PI3K/AKT small molecular inhibitor LY294002 was used to treat cancer cells. Addition of LY294002 in the cell culture significantly suppressed CXCL5-induced PI3K/AKT signaling activation (Fig. 5b). CXCL5-mediated the expression of PD-L1 was decreased after treatment with LY294002 for 48 hr (Fig. 5c and 5d).

To further verify the correlation between the characteristic of CAFs, p-AKT, CXCR2 and PD-L1 *in vivo*, the protein expression of  $\alpha$ -SMA, p-AKT, CXCR2 and PD-L1 in human cancer tissues and xenograft tumor models were examined. CXCR2 was found to be positively correlated with PD-L1 in human melanoma and CRC tissues (Fig. 6a). Even though  $\alpha$ -SMA had no correlation with PD-L1 in xenograft tumor tissues (Supporting Information Fig. S3), both CXCR2 and p-AKT were found to be positively correlated with PD-L1 in xenograft tumor tissues (Fig. 6b–6d). As the illustration in Figure 7, the exposure of melanoma and CRC cancer cell lines to CXCL5, derived by CAFs, activated the PI3K/AKT pathways and in turn, the PI3K/AKT signaling pathways regulated the expression of PD-L1 thereby influencing CXCL5-mediated biological functions.

### Discussion

Accumulating researches have highlighted the crucial role of cancer microenvironment in melanoma and CRC progression, metastasis and evasion of the immune surveillance.<sup>20,21</sup> In this study, we found that the quantity of CAFs in melanoma and CRC were positively correlated with PD-L1 expression. CAFs and the derivation, CXCL5, promoted the expression of PD-L1 in mice melanoma and CRC cancer cells via PI3K/AKT signaling pathways. LY294002 inhibited PI3K/AKT signaling pathways and reversed the PD-L1 expression increased by CXCL5 in turn. These findings revealed a complex tumor-promoting microenvironment shaped by CXCL5–CXCR2 axis in melanoma and CRC.

Evidences have shown the vital role of CAFs in cancer evasion of the immune surveillance, including hepatocellular carcinoma (HCC), esophageal cancer, CRC and melanoma.<sup>14,22,23</sup> It was reported that CAFs secreted cytokines, such as, IL-6, IL-4, IL-8, IL-10, tumor necrosis factor (TNF), TGF- $\beta$ , C-C motif chemokine ligand 2 (CCL2), CCL5, C-X-C motif chemokine ligand CXCL9, CXCL10, CXCL12, have direct and/or indirect implications for tumor immunity.<sup>7,24</sup> Our present study indicated that CAFs were positively correlated with the expression of PD-L1 in human tumor tissues and governed the upregulated PD-L1 expression in mice melanoma and CRC cell lines. Chemokines have been served as the master controllers by modulating nonimmunogenic functions. Interestingly, we identified that the RNA and protein expression of CXCL5 in mice CAFs were significantly increased, while normal mice fibroblasts 3T3 almost did not express. As a confirmation, immunofluorescent staining and IHC showed increased CXCL5 expression in CAFs. In addition, it was demonstrated that non-small cell lung cancer, melanoma and CRC tumor cell lines also highly expressed CXCL5 which mold tumor microenvironment.<sup>17,25,26</sup> Therefore, it seemed that CXCL5 was with diverse origins. Taken together, these data indicated an intriguing effect of CXCL5 in melanoma and CRC tumor microenvironment.

CXCL5 binds CXCR2 to mediate neutrophil recruitment, tumor cell migration and invasion.<sup>25,27</sup> We here showed that CAFs secreted CXCL5 to combine the CXCR2 in the surface of cancer cells. Notably, CXCL5 promoted PD-L1 expression in B16, CT26, A375 and HCT116 in a concentration-dependent manner. Furthermore, the upregulating expression of PD-L1 induced by CAFs reversed after the CXCR2 in tumor cells were silenced. Moreover, the PD-L1 expression in B16 and CT26 were upregulated after cocultured with CXCL5-overexpression fibroblasts, which did not display CAFs properties. CXCL5 also did not increase together with classical CAF markers under

**Figure 5.** CXCL5 promotes PD-L1 expression through PI3K/AKT signaling pathway. (a) B16 and CT26 were treated with CXCL5 for different times in 2 hr and the key proteins of PI3K/AKT signaling pathway were detected via western blot. The normalized protein expression was analyzed by Image J. (b) B16, CT26, A375 and HCT116 were pretreated with or without LY294002 (10  $\mu$ M) for 2 hr and treated with CXCL5 for 1 hr. The protein expression of p-AKT, AKT, p-PI3K and PI3K were detected by western and the corresponding graph was showed. Cells were pretreated with or without LY294002 for 2 hr and treated with CXCL5 for 48 hr. (c) The protein expressions and the corresponding graphs of PD-L1 were detected by western. (d) The PD-L1 expressions were determined by flow cytometry. \* $p < 0.05$ .

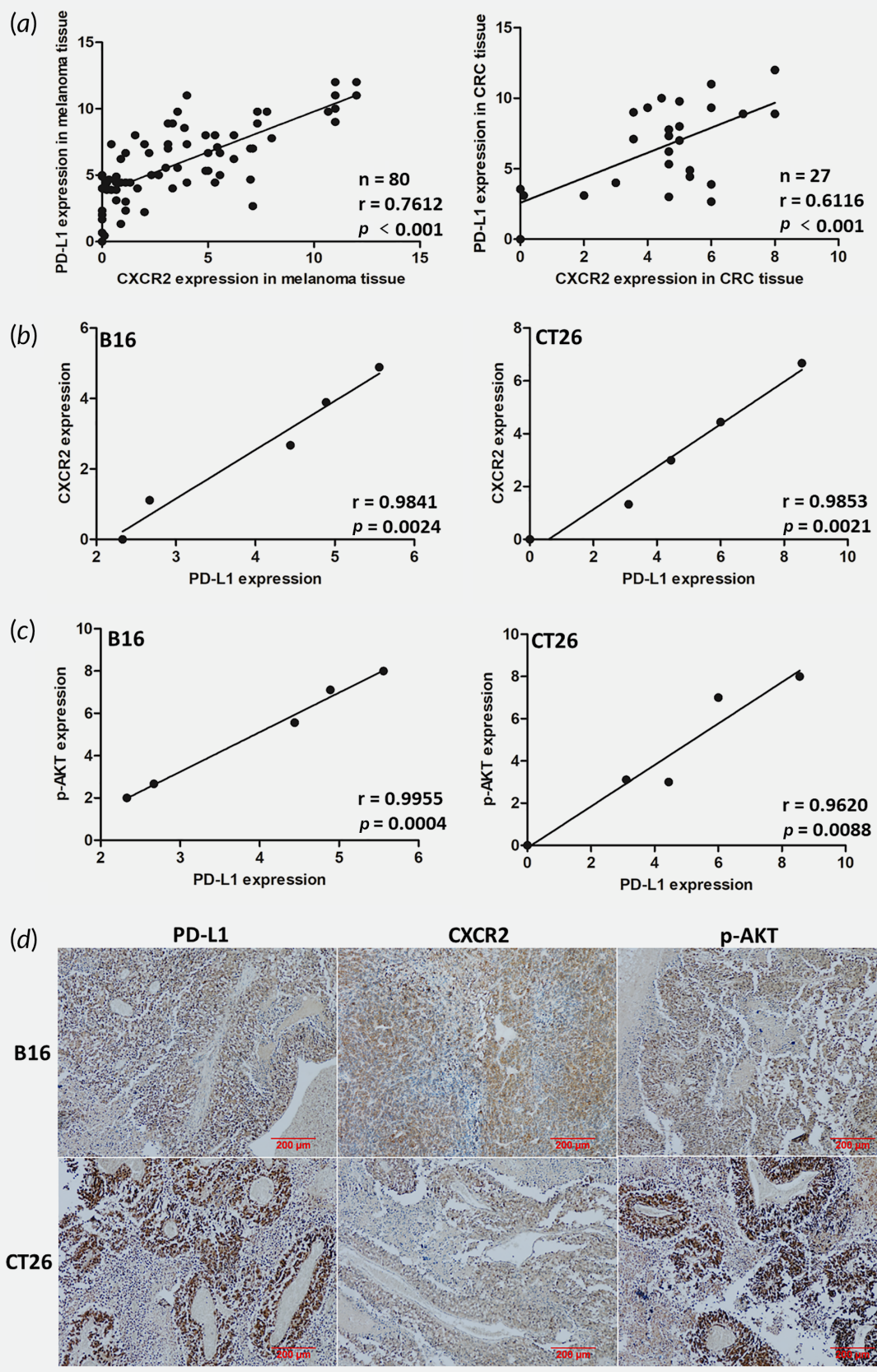


**Figure 6.** The correlation of CXCR2, PD-L1 and p-AKT in tumor tissues *in vivo*. (a) The expression level of CXCR2 and PD-L1 in human melanoma and CRC tissues were detected by IHC and evaluated. (b) The correlation of CXCR2 and PD-L1 in xenograft tumor tissues was analyzed by IHC and evaluated. (c) The correlation of p-AKT and PD-L1 in xenograft tumor tissues was detected by IHC and quantized. (d) Representative immunostaining images of PD-L1, CXCR2 and p-AKT in B16 and CT26 xenograft tumor tissues. Scale bar, 200  $\mu\text{m}$ .

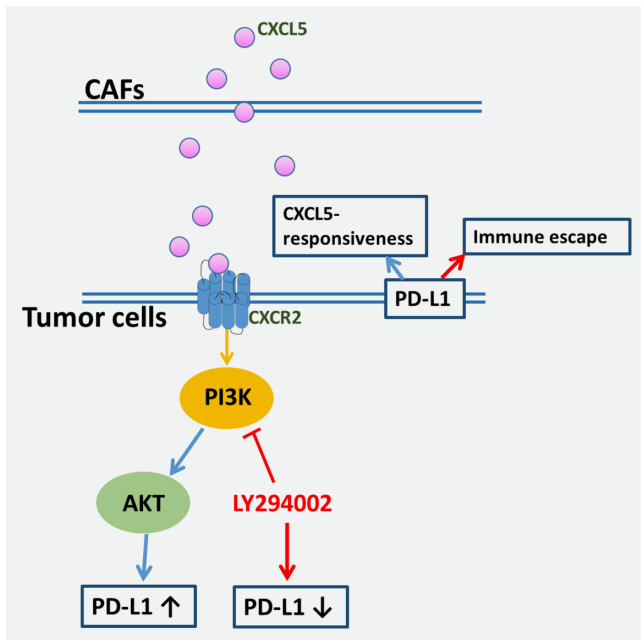


Figure 7. The crosstalk between PD-L1 and PI3K/AKT signaling in melanoma and CRC cells in response to CXCL5.

TGF- $\beta$  treatment, which may be due in large due to the different compositions between CAFs and those fibroblasts activated by cytokines. Because CAFs were reported to be a heterogeneous population of fibroblasts.<sup>28</sup> Nonetheless, since our analyses focused on CAFs derived from tumor tissues, which were observed to express CXCL5 significantly, we suggest that the expression of CXCL5 may be the character rather than the symbol of CAFs in melanoma and CRC. In liver cancer, CXCL5 was reported to be a candidate of diagnostic and therapeutic biomarkers with potential clinical values.<sup>29</sup> Meanwhile, CXCL5 could also attract neutrophil toward melanoma and HCC.<sup>25,30</sup> Therefore, CXCL5 affects the complex tumor microenvironment at multiple ways. In our research, CXCL5 inhibited

antitumor immunity via PD-L1 through activating PI3K and AKT signaling in melanoma and CRC cells. Previous studies have reported that effects of PI3K pathway on PD-L1 expression are complex and variable among cell lines.<sup>31,32</sup> Blocking PI3K/AKT signaling significantly inhibited the upregulating expression of PD-L1 in B16, CT26, A375 and HCT116 induced by CXCL5. Furthermore, the western assay showed that LY294002 also inhibited PD-L1 expression in the normal cancer cells mainly due to other cytokines and factors derived by CAFs and/or tumor cells.

Tumor cells and other mesenchymal cells such as fibroblasts, smooth muscle cells and epithelial cells may secrete CXCL5 under certain conditions.<sup>25</sup> Given CXCL5 signal only through CXCR2, we analyzed correlation between CXCR2 and PD-L1 to illustrate the role of CXCL5/CXCR2 interaction on the expression of PD-L1. In human tumor sections and our mouse model, the expression of PD-L1 was positively correlated with CXCR2 and p-AKT. In our study, evidence showed that  $\alpha$ -SMA had no correlation with PD-L1 in xenograft tumor tissues which was mainly due to the deficiency of cases. The findings illustrated the CXCL5–CXCR2 axis may become a promising therapeutic target to melanoma and CRC patients.

In conclusion, our results described CAFs secreted CXCL5 in tumor environment that promoted PD-L1 expression in mice melanoma and CRC cells. CXCL5 combined with CXCR2 and then activated PI3K/AKT pathway to burst immune inhibitory factor PD-L1. The crosstalks between cancer cells and stromal cells are essential for tumor progression. Thus, the characteristics of CXCL5 in tumor microenvironment strongly support its possibility as a novel therapeutic target. However, extensive research is required for its application.

### Author's Contribution

ZL and JD conceived and designed the experiments and wrote the article. ZL, JZ, JZ and SL performed the experiments and analyzed the data. HW and JD supervised the entire experimental work and discussed the results. All authors have read and approved the final version of the article.

### References

- Fidler MM, Bray F, Soerjomataram I. The global cancer burden and human development: a review. *Scand J Public Health* 2018;46:27–36.
- Mitchell TC, Feld E. Immunotherapy in melanoma. *Immunotherapy* 2018;10:987–98.
- Dosset M, Vargas TR, Lagrange A, et al. PD-L1/PD-L1 pathway: an adaptive immune resistance mechanism to immunogenic chemotherapy in colorectal cancer. *Oncoimmunology* 2018;7:e1433981.
- Arora SP, Mahalingam D. Immunotherapy in colorectal cancer: for the select few or all? *J Gastrointest Oncol* 2018;9:170–9.
- Liao Z, Tan ZW, Zhu P, et al. Cancer-associated fibroblasts in tumor microenvironment—accomplices in tumor malignancy. *Cell Immunol* 2018;17:1–11.
- Ma Z, Chen M, Yang X, et al. The role of cancer-associated fibroblasts in tumorigenesis of gastric cancer. *Curr Pharm Des* 2018;24:3297–302.
- Kalluri R. The biology and function of fibroblasts in cancer. *Nat Rev Cancer* 2016;16:582–98.
- Tao L, Huang G, Song H, et al. Cancer associated fibroblasts: an essential role in the tumor microenvironment. *Oncol Lett* 2017;14:2611–20.
- Andersen BL, Goyal NG, Weiss DM, et al. Cells, cytokines, chemokines, and cancer stress: a biobehavioral study of patients with chronic lymphocytic leukemia. *Cancer Am Cancer Soc* 2018;124:3240–8.
- Gao D, Fish EN. Chemokines in breast cancer: regulating metabolism. *Cytokine* 2018;109:57–64.
- Goltz D, Holmes EE, Gevensleben H, et al. CXCL12 promoter methylation and PD-L1 expression as prognostic biomarkers in prostate cancer patients. *Oncotarget* 2016;7:53309–20.
- Gao Y, Yang J, Cai Y, et al. IFN-gamma-mediated inhibition of lung cancer correlates with PD-L1 expression and is regulated by PI3K-AKT signaling. *Int J Cancer* 2018;143:931–43.
- Zhang C, Li Z, Xu L, et al. CXCL9/10/11, a regulator of PD-L1 expression in gastric cancer. *BMC Cancer* 2018;18:462.
- Cheng Y, Li H, Deng Y, et al. Cancer-associated fibroblasts induce PDL1+ neutrophils through the IL6-STAT3 pathway that foster immune suppression in hepatocellular carcinoma. *Cell Death Dis* 2018;9:422.
- Li Z, Chan K, Qi Y, et al. Participation of CCL1 in snail-positive fibroblasts in colorectal cancer contribute to 5-fluorouracil/paclitaxel chemoresistance. *Cancer Res Treat* 2018;50:894–907.
- Liu LZ, Zhang Z, Zheng BH, et al. CCL15 recruits suppressive monocytes to facilitate immune escape and disease progression in hepatocellular carcinoma. *Hepatology* 2019;69:143–59.
- Wu K, Yu S, Liu Q, et al. The clinical significance of CXCL5 in non-small cell lung cancer. *Onco Targets Ther* 2017;10:5561–73.

18. Coelho MA, de Carné Trécesson S, Rana S, et al. Oncogenic RAS signaling promotes tumor immunoresistance by stabilizing PD-L1 mRNA. *Immunity* 2017;47:1083–99.
19. Park BV, Freeman ZT, Ghasemzadeh A, et al. TGF 1-mediated SMAD3 enhances PD-1 expression on antigen-specific T cells in cancer. *Cancer Discov* 2016;6:1366–81.
20. Giavina-Bianchi MH, Giavina-Bianchi PJ, Festa CN. Melanoma: tumor microenvironment and new treatments. *An Bras Dermatol* 2017;92:156–66.
21. Zhang L, Zhao Y, Dai Y, et al. Immune landscape of colorectal cancer tumor microenvironment from different primary tumor location. *Front Immunol* 2018;9:1578.
22. Kato T, Noma K, Ohara T, et al. Cancer-associated fibroblasts affect intratumoral CD8(+) and FoxP3(+) T cells via IL6 in the tumor microenvironment. *Clin Cancer Res* 2018;24:4820–33.
23. Anari F, Ramamurthy C, Zibelman M. Impact of tumor microenvironment composition on therapeutic responses and clinical outcomes in cancer. *Future Oncol* 2018;14:1409–21.
24. Feig C, Jones JO, Kraman M, et al. Targeting CXCL12 from FAP-expressing carcinoma-associated fibroblasts synergizes with anti-PD-L1 immunotherapy in pancreatic cancer. *Proc Natl Acad Sci USA* 2013;110:20212–7.
25. Forsthuber A, Lipp K, Andersen L, et al. CXCL5 as regulator of neutrophil function in cutaneous melanoma. *J Invest Dermatol* 2019;139:186–94.
26. Zhao J, Ou B, Han D, et al. Tumor-derived CXCL5 promotes human colorectal cancer metastasis through activation of the ERK/Elk-1/snail and AKT/GSK3 $\beta$ /catenin pathways. *Mol Cancer* 2017;16:70.
27. Qiu WZ, Zhang HB, Xia WX, et al. The CXCL5/CXCR2 axis contributes to the epithelial-mesenchymal transition of nasopharyngeal carcinoma cells by activating ERK/GSK-3 $\beta$ /snail signalling. *J Exp Clin Cancer Res* 2018;37:85.
28. Nurmik M, Ullmann P, Rodriguez F, et al. In search of definitions: cancer-associated fibroblasts and their markers. *Int J Cancer* 2019;1–11.
29. Xia J, Xu X, Huang P, et al. The potential of CXCL5 as a target for liver cancer—what do we know so far? *Expert Opin Ther Targets* 2015;19:141–6.
30. Xu X, Huang P, Yang B, et al. Roles of CXCL5 on migration and invasion of liver cancer cells. *J Transl Med* 2014;12:193.
31. Haider C, Hnat J, Wagner R, et al. Transforming growth factor-beta and Axl induce CXCL5 and neutrophil recruitment in hepatocellular carcinoma. *Hepatology* 2018;68:S674–5.
32. Atefi M, Avramis E, Lassen A, et al. Effects of MAPK and PI3K pathways on PD-L1 expression in melanoma. *Clin Cancer Res* 2014;20:3446–57.